Computer-Aided Design 78 (2016) 26–35

Contents lists available at ScienceDirect

Computer-Aided Design

journal homepage: www.elsevier.com/locate/cad

Tool path generation for chamfering drill holes of a pipe with constant width

Takato Sato [a], Youichi Sato [b], Takashi Maekawa [a,*]

[a] Department of Mechanical Engineering, Yokohama National University, Japan

[b] Xebec Technology, Japan

ARTICLE INFO

Keywords:
Constant chamfering
Differential geometry
Intersection curve
Cutter interference

ABSTRACT

When drilling circular holes into metal circular pipes, burr is generated at the hole entrance as well as at the hole exit. The burrs generated at the edge curves associated with the outer and inner pipe surfaces must be removed by constant chamfering. Geometrically, the two edge curves can be defined as cylinder-to-pipe intersection curves. In this paper, we employ differential geometric properties of the surface-to-surface intersection curves in order to generate an interference-free tool path with constant chamfering for a ball-end cutter. We demonstrate the effectiveness of our method by conducting experiments with physical pipe models.

1. Introduction

Burr is formed as a result of the undesirable plastic flow of metals through various machining operations applied to tasks such as grinding, drilling, milling, engraving, and turning [1]. Burr may cause injury to workers during the assembly process, and may trigger severe problems in high-speed equipment, fluid-power systems, food processing, etc. [1]. Therefore, deburring must be included in the finishing process not only to remove the unwanted burr, but also to ensure uniform chamfering at the produced edges for aesthetic purposes. It is also known that constant chamfering can greatly improve the performance and lifetime of products [1]. Unfortunately, the most common burr removal process currently employed in manufacturing plants is hand deburring using hand-held deburring tools, which is time consuming [1]. Furthermore, there is no chamfer on the curved edge. According to Gillespie [2], for precision parts, edge finishing frequently constitutes 30% of the overall cost. Liao et al. [3] proposed the modeling and control of an automated polishing/deburring process that utilizes a dual-purpose compliant toolhead. However, the problem of tools interfering with work was not discussed. Song and Song [4] studied a tool path modification method using an iterative closest point (ICP) based contour matching algorithm to enable the robotic deburring process to compensate for the position/orientation errors of the workpiece when it is placed in a jig. The proposed method was implemented on a six degree of freedom (DOF) articulated manipulator with force control strategies and a virtual wall to perform the robotic deburring. However, the quality of the deburring was not discussed.

In this paper, we introduce an interference-free automatic tool path generation method for a ball-end cutter with constant chamfering to remove burrs resulting from the drilling of a circular pipe based on the differential geometry of cylinder-to-pipe intersection curves. As shown in Fig. 2(a), the resulting intersection curve is a space curve, which looks like the curved edge of a potato chip. We assume that the drilling operation is perpendicular to the pipe without eccentricity, and a tool consists of a ball-end cutter and a circular rod, which must not interfere with the pipe, with the exception of the cutter contact point, while deburring.

The remaining part of this paper is organized as follows. In Section 2, we present the differential geometry of the cylinder-to-pipe intersection curves. The tool path generation for the deburring process is discussed in Section 3. In Section 4, we study cutter interference avoidance. In Section 5, we demonstrate the effectiveness of our method by conducting experiments using physical pipe models. Finally, we conclude the paper in Section 6.

2. Differential geometry of cylinder-to-pipe intersection curves

We first introduce several notations and definitions. Bold letters such as $\mathbf{t}$, $\mathbf{C}(\theta)$ denote vectors and vector functions. Equivalently, (a, b, c) and $(a(\theta),\ b(\theta),\ c(\theta))$ denote vectors and vector functions, respectively. The dot $\dot{\mathbf{C}}(\theta)$ denotes the differentiation of $\mathbf{C}(\theta)$ with respect to the parameter θ.

* Corresponding author. Tel.: +81 45 339 3930.
E-mail address: maekawa@ynu.ac.jp (T. Maekawa).

http://dx.doi.org/10.1016/j.cad.2016.04.008
0010-4485/

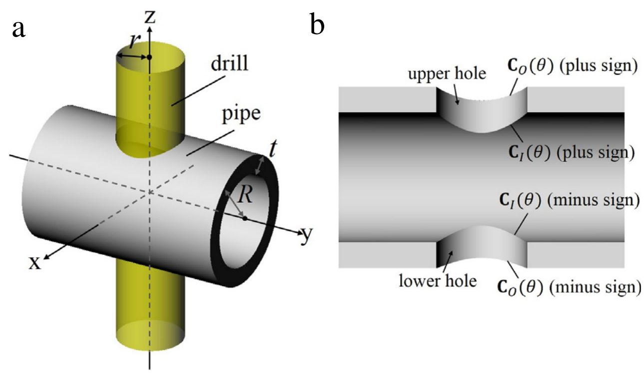

Fig. 1. (a) A drill (cylinder) intersects a circular pipe orthogonally without eccentricity. (b) Four intersection curves.

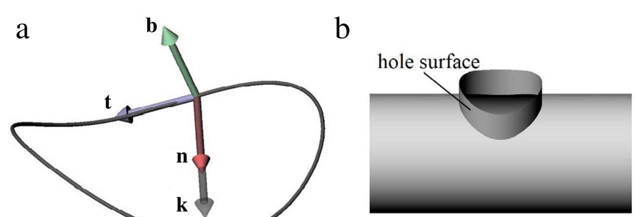

Fig. 2. Cylinder-to-pipe intersection: (a) Frenet frame along the intersection curve. The intersection curve looks like the edge of a potato chip. (b) The hole surface spanned by the two intersection curves is a ruled surface.

2.1. Cylinder-to-pipe intersection curve

Let us define a mathematical description of the geometry, which is illustrated in Fig. 1(a). In this paper, we consider the geometry of a cylinder-to-pipe intersection where a circular pipe consisting of outer and inner surfaces with thickness t are intersected orthogonally without eccentricity by a circular cylinder representing a drill. In other words, the center lines of the pipe and drill intersect orthogonally. We assume that the drill is represented by a cylinder having a radius r, and its centerline coincides with the z-axis. It can be expressed by a parametric form:

$$\mathbf{D}(\theta, z) = (r\cos\theta,\ r\sin\theta,\ z), \tag{1}$$

where θ is the parameter within $0 \le \theta \le 2\pi$. We take the center line of the outer pipe surface, which is coincident with the y-axis, having a radius R, and represent it by an implicit form:

$$x^2 + z^2 = R^2. \tag{2}$$

Similarly, the inner pipe surface is given by

$$x^2 + z^2 = {R_I}^2, \tag{3}$$

where $R_I = R - t$ is the radius of inner pipe surface and t is the pipe thickness. We can obtain the intersection curves $\mathbf{C}_O(\theta)$ between the drill surface and the outer pipe surface by substituting the vector components of (1) into (2), and solving for z, which yields a parametric representation of the intersection curve [5,6]:

$$\mathbf{C}_O(\theta) = \left(r\cos\theta,\ r\sin\theta,\ \pm\sqrt{R^2 - r^2\cos^2\theta}\right), \tag{4}$$

where the plus sign corresponds to the upper intersection curve, while the minus sign corresponds to the lower intersection curve (see Fig. 1(b)). In this paper, we only consider the upper intersection curve (plus sign), as the minus sign can be obtained in the same manner. Similarly, we have two intersection curves $\mathbf{C}_I(\theta)$ for the inner pipe surface:

$$\mathbf{C}_I(\theta) = \left(r\cos\theta, r\sin\theta, \pm\sqrt{{R_I}^2 - r^2\cos^2\theta}\right), \tag{5}$$

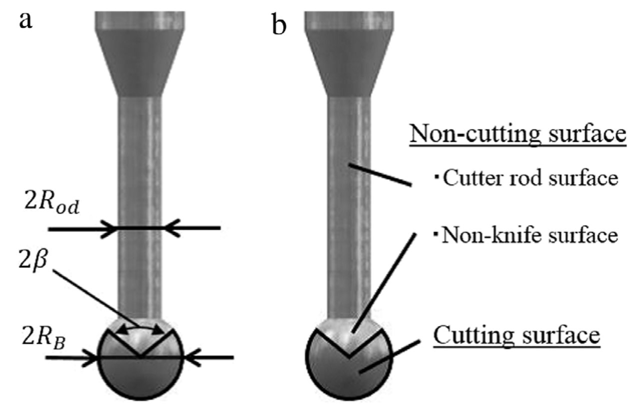

Fig. 3. Ball-end cutter: (a) Geometry. (b) Classification of the ball-end cutter surface.

where we only consider the upper intersection curve (plus sign) (see Fig. 1(b)). To simplify the notation, we drop the subscripts O, I from $\mathbf{C}$ throughout the rest of the paper, except when stated otherwise.

2.2. Differential geometry of intersection curve

The unit tangent $\mathbf{t}$, binormal $\mathbf{b}$, and normal $\mathbf{n}$ vectors of the intersection curve $\mathbf{C}(\theta)$ (see Fig. 2(a)) can be obtained as

$$\mathbf{t} = \frac{\dot{\mathbf{C}}(\theta)}{|\dot{\mathbf{C}}(\theta)|}, \tag{6}$$

$$\mathbf{b} = \frac{\dot{\mathbf{C}}(\theta) \times \ddot{\mathbf{C}}(\theta)}{|\dot{\mathbf{C}}(\theta) \times \ddot{\mathbf{C}}(\theta)|}, \tag{7}$$

$$\mathbf{n} = \mathbf{b} \times \mathbf{t}. \tag{8}$$

The curvature of the intersection curve is given by

$$\kappa = \frac{|\dot{\mathbf{C}}(\theta) \times \ddot{\mathbf{C}}(\theta)|}{|\dot{\mathbf{C}}(\theta)|^3}, \tag{9}$$

and the curvature vector $\mathbf{k}$ is obtained as

$$\mathbf{k} = \kappa\mathbf{n}. \tag{10}$$

3. Tool path generation

3.1. Hole surface

The hole surface $\mathbf{H}(\theta, \tau)$ (see Fig. 2(b)) is a ruled surface bounded by two intersection curves $\mathbf{C}_I(\theta)$ and $\mathbf{C}_O(\theta)$, and is defined as follows:

$$\mathbf{H}(\theta, \tau) = (1-\tau)\mathbf{C}_I(\theta) + \tau\mathbf{C}_O(\theta). \tag{11}$$

The unit normal vector of the hole surface $\mathbf{N}_H$ is simply a unit normal of a cross-sectional circle of the cylinder representing the drill, and it is given by

$$\mathbf{N}_H = (\cos\theta,\ \sin\theta,\ 0)\,. \tag{12}$$

3.2. Ball-end cutter

The deburring cutter consists of double-start knife edges wrapped around a sphere of diameter $2R_B$ in the form of a right-handed helix with a lead angle 15°, and it is connected to a rod of diameter $2R_{od}$, as illustrated in Fig. 3(a). The knife edge of the cutter is limited to the angle $360° - 2\beta$, as depicted in Fig. 3(a). The non-cutting surface consists of the non-knife and cutter rod surfaces, as illustrated in Fig. 3(b). The ball-end cutter is attached to a compact machining center (DMG Mori Seiki MILLTAP 700) that is equipped with a vertical 3-axis milling.